

## Monitoring the Monsoon in the Himalayas: Observations in Central Nepal, June 2001

ANA P. BARROS AND TIMOTHY J. LANG

*Division of Engineering and Applied Sciences, Harvard University, Cambridge, Massachusetts*

(Manuscript received 5 August 2002, in final form 5 December 2002)

### ABSTRACT

The Monsoon Himalayan Precipitation Experiment (MOHPREX) occurred during June 2001 along the south slopes of the Himalayas in central Nepal. Radiosondes were launched around the clock from two sites, one in the Marsyandi River basin on the eastern footholds of the Annapurna range, and one farther to the southwest near the border with India. The flights supported rainfall and other hydrometeorological observations (including surface winds) from the Marsyandi network that has been operated in this region since the spring of 1999. The thermodynamic profiles obtained from the soundings support the observed nocturnal maximum in rainfall during the monsoon, with total column moisture and instability maximized just before rainfall peaks. Coinciding with the appearance of a monsoon depression over central India, the onset of the monsoon in this region was characterized by a weeklong weakening of the upper-level westerlies, and an increase in moisture and convective instability. The vertical structure of convection during the project was intense at times, and frequent thunder and lightning were observed. This is suggestive of monsoon break convection, which is expected to be predominant since the monsoon had not fully matured by the end of the month. Comparisons of the MOHPREX data with the NCEP-NCAR reanalysis data reveal that upper-level winds are characterized relatively well by the reanalysis, taking into account the coarse model topography. However, moisture is severely underestimated, leading to significant underestimation of rainfall by the reanalysis. The interaction of the ambient monsoon flow with the south slopes of the Himalayas, modulated by the diurnal variability of atmospheric state, is suggested as the primary cause of the nocturnal peak in rainfall.

### 1. Introduction

#### *Background*

Atmospheric structure and hydrometeorological processes along the south slopes of the Himalayas are not well known or well documented, mainly because of the rugged and remote terrain. Also, the mountain range lies within several poor, developing countries, such as Nepal, that do not have the resources to carry out sophisticated meteorological studies. For example, before 2001 no radiosondes had been launched in Nepal for more than 20 yr (M. L. Shrestha, Nepal Department of Hydrology and Meteorology, 2002, personal communication).

Despite these difficulties, however, it is becoming clear that many interesting and important atmospheric phenomena occur in this region. Recent studies have shown that large rainfall amounts, on the order of 300–400 cm yr<sup>-1</sup>, can fall along the south-facing slopes of the Himalayas (Barros et al. 2000; Shrestha 2000; Lang and Barros 2002). Studies also have shown that the climatology of Himalayan rainfall variability differs

markedly from the rest of the Indian subcontinent (Shrestha et al. 2000). The hydrological importance of this rainfall is substantial, as the rivers spawned in the central Himalayas are tributaries to the Ganges River, which is a critical water supply for hundreds of millions of people. In addition, the landslides and erosion caused by this rainfall suggest important geomorphologic impacts (Burbank and Pinter 1999).

There have been several studies on the large-scale effects of the Himalayas and Tibetan Plateau on the Asian summer monsoon (e.g., Ye 1981; Luo and Yanai 1983, 1984; Chen et al. 1985; He et al. 1987; Li and Yanai 1996; Wu and Zhang 1998, among others), as well as their effects on the diurnal circulation in the monsoon region (e.g., Kuo and Qian 1981; Krishnamurti and Kishtawal 2000). One thing these studies show is that convection in the Himalayas and Tibetan Plateau plays an important role in sustaining the monsoon, through the release of latent heat. Unfortunately, these studies have not expressly focused on the south-facing slopes of the Himalayas, where rainfall has not been well quantified until recent years. The modulating effect of south-slope rainfall on the latent heating of the regional atmosphere (Magagi and Barros 2003, hereafter MB) and how that impacts the Asian summer monsoon are still unclear, but likely are very important given the large rainfall totals.

---

*Corresponding author address:* Dr. Ana P. Barros, Division of Engineering and Applied Sciences, Harvard University, Pierce Hall 118, 29 Oxford St., Cambridge, MA 02138.  
E-mail: barros@deas.harvard.edu

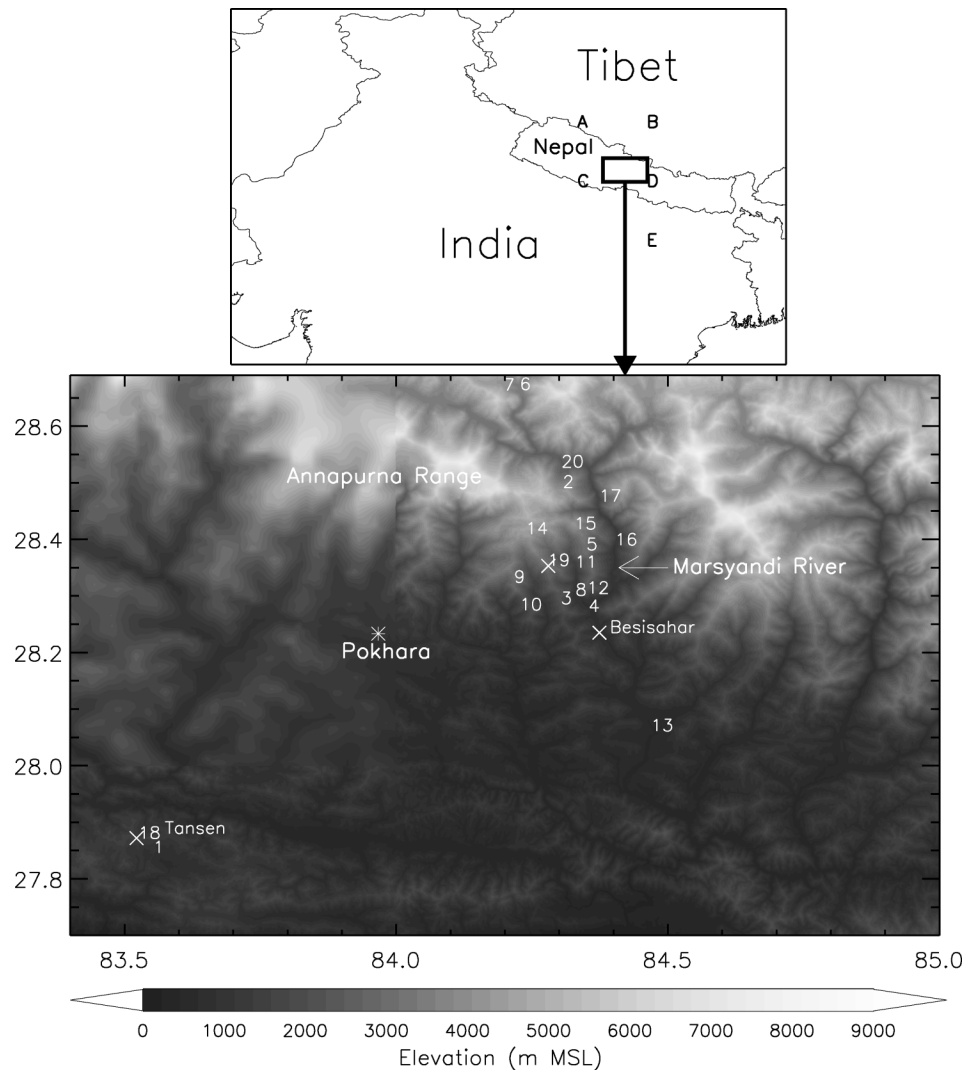


FIG. 1. Topographic map of the Marsyandi River basin, showing locations of the meteorological stations in the network (numbers; Table 1) as well as the MOHPREX radiosonde launch locations and the Telbrung micrometeorological tower (Xs). Also shown are various landmarks in the region, including the city of Pokhara. The large-scale map shows the location of the network relative to southern Asia, as well as the locations of the grid points used in the NCEP–NCAR reanalysis comparison (letters; Table 3).

The question of rainfall impacts in this region and its surroundings is especially pertinent given that past studies of rainfall in this region, largely based on remote sensing and valley rain gauges, tend to underestimate seasonal totals, particularly for high-altitude ridges (Barros et al. 2000).

#### *b. The Marsyandi hydrometeorological network*

A hydrometeorological network was installed in the Marsyandi River basin in central Nepal during the spring of 1999 (Barros et al. 2000). This network lies on several ridges and valleys along the eastern slopes of the Annapurna Range (Fig. 1; Table 1). Beside the aforementioned rainfall totals, both Barros et al. (2000)

and Lang and Barros (2002) noted significant spatial variability in precipitation (factor of  $\sim 4$  differences over  $\sim 10$  km distance), which did not show any specific dependence on elevation, particularly at the seasonal scale. In addition, Barros et al. (2000) noted an interesting nocturnal peak in rainfall, just past midnight. Other researchers have noted this regional phenomenon as well (Ohsawa et al. 2001; Ueno et al. 2001; Yatagai 2001; Bollasina et al. 2002). This is unusual for mountainous regions, which often show an afternoon peak (see Banta 1990 for a review) associated with diurnally forced upslope flow. While such a peak is visible in the data (Barros et al. 2000), it often is secondary, particularly at low elevations. One of the more interesting facets of the nocturnal rainfall peak is that it exists most

TABLE 1. Summary of Marsyandi meteorological network: JJAS, 1 Jun–30 Sep. NA, not available. Station type: H (high altitude  $\geq$  2000 m), L (low altitude  $<$  2000 m), D (dry station in lee of Annapurnas).

Station no. and name	Type	Elevation (m MSL)	Jun 2001 rain (mm)	2001 JJAS rain (mm)
1) Bortung	L	1072	256	1144
2) Danfedanda	H	3987	325	1550
3) Ganpokhara	H	2120	868	3162*
4) Khudi	L	820	696	2312
5) Koprung	H	3133	593	2797
6) Monastery	D	3562	NA	NA
7) Nargaon	D	4220	NA	NA
8) Paiyu Khola	L	993	671	2786
9) Pasqam Ridge	H	2950	974	4279
10) Pasqam Village	L	1702	NA	NA
11) Probi	L	1495	529	2612
12) Purano Village	L	1787	681	790*
13) Purkot	L	528	338	1287
14) Rambrong	H	4435	206*	2023*
15) Sundar	H	3823	694	2854
16) Syange	L	1200	516	2117
17) Tal	L	1358	292	1292
18) Tansen	L	1521	301	1469
19) Telbrung	H	3168	784	3532
20) Temang	D	2760	175	821

\* Incomplete record during MOHPREX/2001 monsoon.

strongly during the summer monsoon; during other times of the year the afternoon peak is predominant. This phenomenon is also observed elsewhere in the Himalayas (Ueno et al. 2001).

Monsoon onset in Nepal can be caused by a Bay of Bengal depression that produces very heavy and sustained rainfall over 2–3 days (Lang and Barros 2002a). Rainfall at certain Marsyandi stations can exceed 30–40 cm and account for 10%–20% of seasonal totals, particularly at high altitudes ( $\geq$ 2000 m MSL). In addition, very strong spatial gradients in rainfall occur, of the same order as those that occur on the seasonal scale.

Egger et al. (2000) reported on a field project that studied the diurnal cycle of winds in the Kali Gandaki valley (just west of the Marsyandi). They noted an asymmetry in diurnal winds, with daytime upvalley winds strongly predominating over weak nocturnal downvalley flow. Other researchers have noted similar phenomena in the Khumbu Valley near Mount Everest (Ueno et al. 2001; Bollasina et al. 2002), with the daytime asymmetry strongest during the monsoon. An interesting question is whether this asymmetry holds in the narrow valleys and convoluted orography that make up most of the Himalayan range, such as the Marsyandi valley.

It is in this context of pronounced spatial and temporal variability of precipitation and winds that the Monsoon Himalayan Precipitation Experiment (MOHPREX) was conceived. The design, goals, and principal results of MOHPREX will be reported upon in this paper.

TABLE 2. Numbers of radiosonde launches for both sites on each day of the MOHPREX project.

Local date (Jun 2001)	Besisahar	Tansen
4	2	
5	2	1
6	2	2
7	6	2
8	6	5
9	5	4
10	6	5
11	6	3
12	6	
13	7	
14	8	
15	8	
16	8	
17	8	
18	7	
19	5	
20	5	
21	5	
22	5	
23	5	
24	5	
25	3	
26	1	

## 2. Design and implementation of MOHPREX

MOHPREX occurred during the period 3–25 June 2001. The principal goal was to characterize and understand the spatial and temporal variability of precipitation along the south-facing slopes of the Himalayas. The variability of precipitation in this region is described by using data from the preexisting hydrometeorological network, as well as the Tropical Rainfall Measuring Mission (TRMM; Kummerow et al. 1998) and *Meteosat-5* (EUMETSAT 2000) satellites. However, understanding of the mechanisms behind this variability requires further information on the basic state of the atmosphere, which can be used to formulate hypotheses that can be tested by future numerical simulations. Hence, the main focus of MOHPREX was the launching of radiosondes.

The design of the project focused on key goals: 1) improved understanding of the diurnal cycle of precipitation, 2) improved understanding of the evolution of the atmosphere during monsoon onset, 3) improved understanding of regional-scale spatial variability of monsoon weather in and near the Himalayas, and 4) improved understanding of the coupling between the monsoon and the hydrological cycle at high elevations in the central Himalayas (not addressed in this manuscript). To help accomplish these goals, two radiosonde launch sites were defined: Besisahar and Tansen (Fig. 1).

Besisahar was designated as the main site, and the vast majority of balloon flights took place there (Table 2). This site is within the north–south-aligned Marsyandi River valley at 785 m MSL, with ridges in excess of 2000 m MSL on either side. The surrounding to-

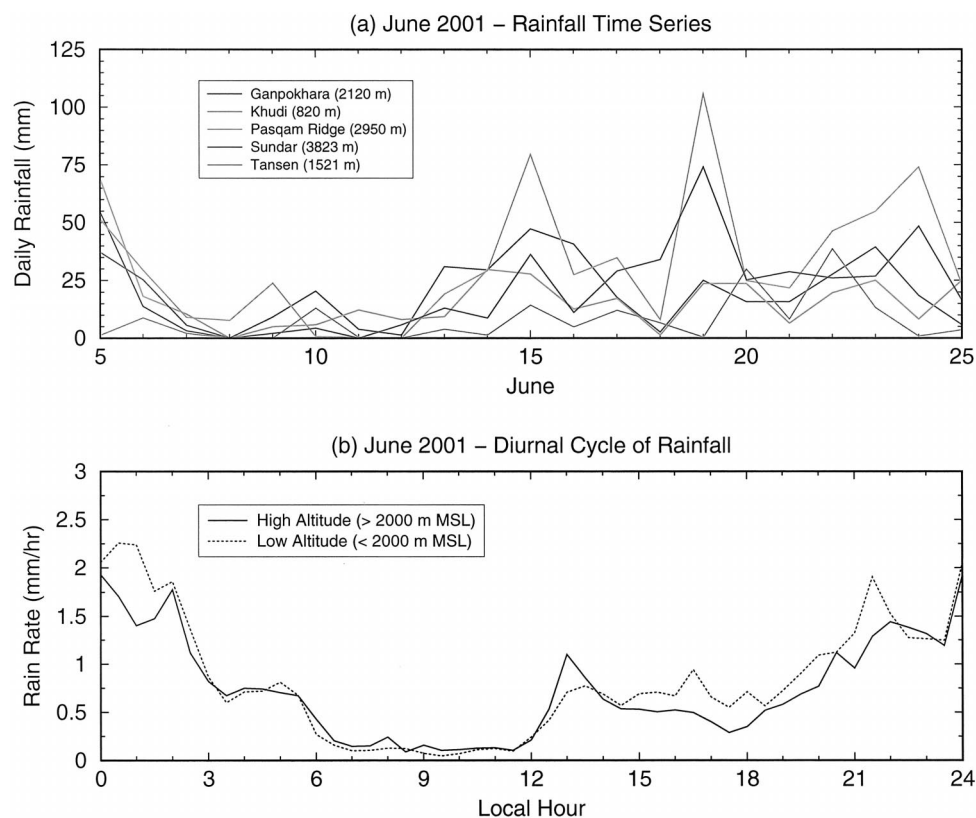


FIG. 2. (a) Time series of daily rainfall during Jun 2001, for selected network stations. (b) Jun 2001 mean diurnal cycle of rainfall for high- and low-altitude gauge stations.

pography forms part of the footslopes of the Annapurna Range, to the northwest. The main advantages of Besisahar were its proximity to the core of the meteorological network (e.g., a gauge station in the town of Khudi lies just a few kilometers up the Annapurna trekking trail), and that it had access to good infrastructure (e.g., paved roads, commercial power, and reasonable accommodations for project workers). Tansen lies 90 km to the southwest (SW) of Besisahar, providing an intermediate location between the mountains and the plains of northern India. The launching site was located near the top of a small, relatively isolated mountain at 1453 m MSL.

The basic frequency of flights, observed at both sites, was five per day: 0000, 0600, 1200, 1800, and 2100 UTC. See Table 2 for launch frequency at both sites. Launches were done on UTC time to better match operational radiosonde observations and model analyses. Nepal is 0545 ahead of UTC time, so this corresponds to 6-hourly flights with one additional nocturnal flight (2100 UTC, or 0245 LNT) to provide more resolution around the time of the postmidnight peak in rainfall. In this case, the 1800 UTC launch precedes this peak, and the 2100 UTC follows it. Launch times periodically were adjusted to match overflights by the TRMM satellite, and at times more than five launches per day (at Besisahar) were made as interesting weather conditions

developed. When monsoon onset occurred (later shown to be after 10 June) launch frequency was increased to 3 hourly (0000, 0300, 0600 UTC, etc.) at Besisahar to better resolve the incoming monsoon flow. This also provided more detailed resolution of the atmospheric diurnal cycle.

Nepal provided many challenges in order to complete a successful field project. Apart from the typical problems associated with developing countries, such as extra logistical strains, poor accommodations, and illness, there were difficult political barriers. The government-mandated mourning period following the tragic demise of the king and queen of Nepal just as MOHPREX was slated to start delayed the project. For the first few days, all launches had to be done late at night, resulting in a low frequency of at most two flights per day (Table 2). Information on sounding data quality control can be found in appendix A.

### 3. Monsoon onset

Daily rainfall at five network stations is shown in Fig. 2a. Monthly and seasonal totals can be found in Table 1. Unlike the previous 2 yr, there was no major rain event associated with the monsoon onset, where  $100+\text{mm day}^{-1}$  of rainfall fell at a majority of the stations over 2 days (Lang and Barros 2002). Indeed, after some

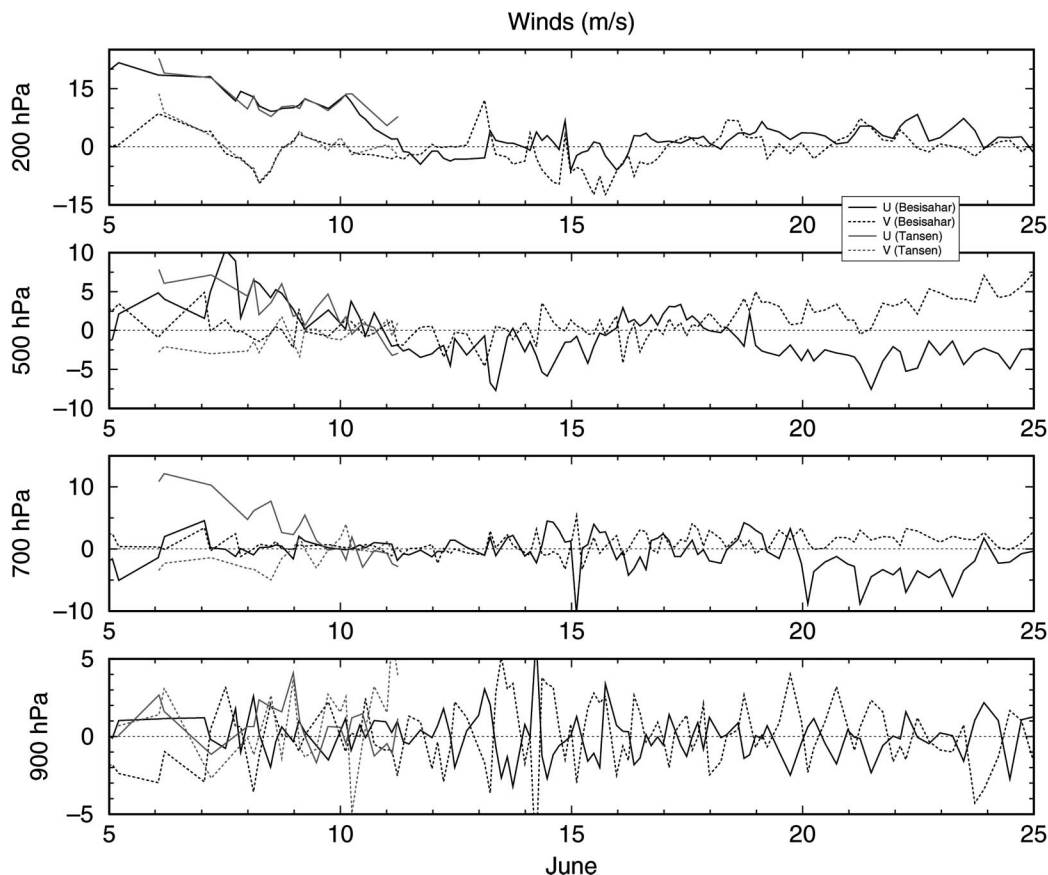


FIG. 3. Time series of Besisahar and Tansen winds at four different atmospheric layers.

significant early rainfall, the weather was relatively dry until 13 June. The most intense storms after this date (15, 19, and 24 June) produced rainfall accumulations up to 100 mm in 1 day, but this was a local phenomenon restricted to one to two gauges at most. However, rainfall was persistent after 12 June, with most gauges receiving at least some rainfall each day.

Average daily rainfall during June 2001 was 17.0 mm at high altitudes and 19.3 mm at low altitudes. Ten of the 17 functioning network gauges during this month received over 500 mm of rain in June (Table 1). The westernmost ridge station (Pasqam Ridge) received 974 mm, the most of any gauge. Khudi (closest to Besisahar) received 696 mm, but the Tansen rain gauge received only 301 mm. The observed rain totals during June 2001 were overall lower when compared with previous years (1999 and 2000). For example, Khudi received 771 mm in June 1999 and 981 mm in 2000, while Tansen had 456 mm in June 1999 and 608 mm in 2000. The primary reason for this was the lack of a major onset rainfall event in 2001 (Lang and Barros 2002).

Figure 3 shows the temporal evolution of horizontal winds at Besisahar and Tansen from four atmospheric layers, centered on 900, 700, 500, and 200 hPa. Nomenclature and sign convention are standard, with pos-

itive  $U$  being westerly flow and positive  $V$  being southerly flow. The data show that the wind profile underwent considerable layer-dependent evolution during June as the monsoon established itself. For instance, being dominated by the diurnal cycle, near-surface winds (900 hPa) at Besisahar exhibited no obvious change throughout the 3 weeks of the project, routinely switching between southeast (SE) flow during the day to northwest (NW) flow at night. Tansen also showed considerable variability but no long-term trends.

At 700 hPa, winds were extremely light during early June, but showed more fluctuations in intensity during the middle of the month. Eventually, ESE flow settled in Besisahar, though with strong variability in intensity [east (E) flow being strongest in the morning]. At Tansen, however, NW winds became increasingly weaker. Note that Tansen is more exposed at 700 hPa than Besisahar, which is situated very close to several 2000–3000-m ridges on the foothills of the Himalayan range (Fig. 1). These ridges serve as an obstacle to flow that does not have a significant southerly component. When mesoscale depressions originating from the Bay of Bengal interact with easterly vertical shear forced by the mountains, an asymmetric secondary circulation develops with strong near-surface upslope (southerly) flow

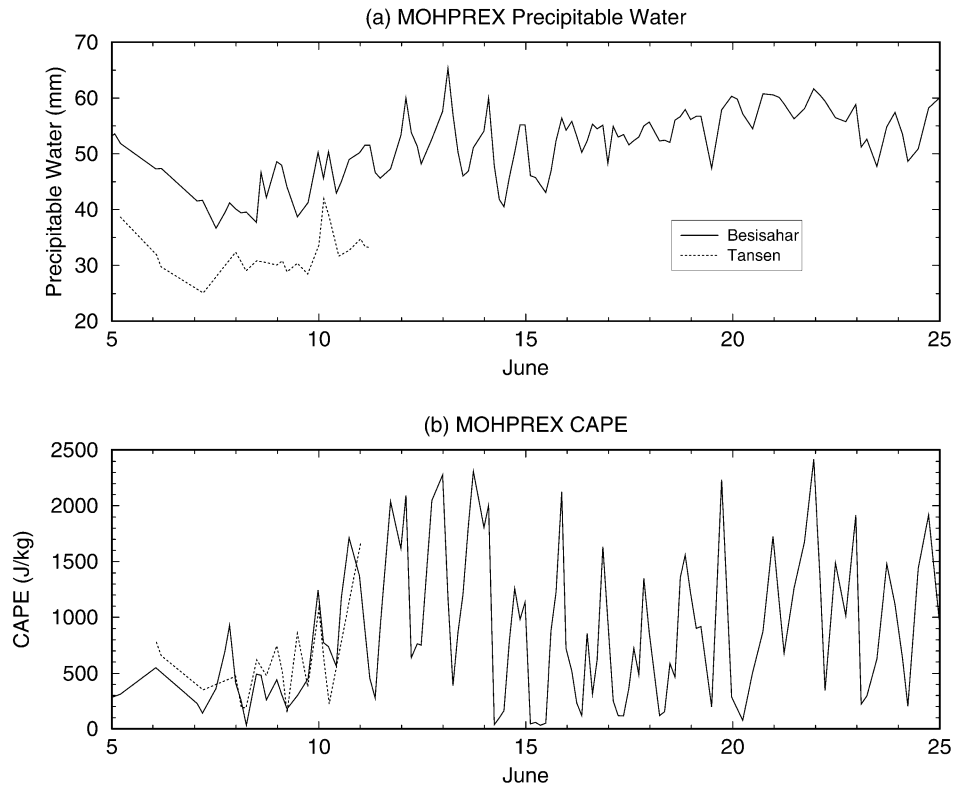


FIG. 4. (a) Time series of Besisahar and Tansen precipitable water. (b) Same as in (a) but for CAPE.

and return flow (northerly) at midlevel (see also Fig. 6 in Lang and Barros 2002).

The largest wind changes occurred aloft at 500 and 200 hPa at Besisahar (nearly perfect agreement with Tansen at 200 hPa). At 500 hPa, winds originally with a significant westerly component vanished after 10 June, becoming more easterly. A short-duration return to light westerly flow occurred after 15 June, but this soon was replaced by well-developed SE flow. The most dramatic reduction in westerly flow occurred at 200 hPa with a decrease in wind velocity from  $U > 20 \text{ m s}^{-1}$  at the beginning of the project to near zero after 11 June. Light and variable westerly flow eventually prevailed toward the end of the month. The north–south component at 200 hPa was variable throughout MOHPREX. The overall impression given by Fig. 3 is that of a reduction in the strength of the westerly component of flow, if not an outright switch to SE winds as the monsoon established itself.

The time evolution of precipitable water (PW) at Besisahar and Tansen is shown in Fig. 4a. While the diurnal cycle was a major component of PW variability, a significant increase in the mean value of PW between 10 and 15 June, remaining more or less constant after that. A similar pattern was found in the values of convective available potential energy (CAPE; Fig. 4b), a measure of atmospheric instability (Moncrieff and Miller 1976). Finally, the atmosphere warmed during the project, with

an increase in freezing-level altitude on the order of 500 m prior to 15 June (not shown).

Based on all these data, it is apparent that monsoon onset occurred during the period 10–15 June, manifesting itself in all notable fields (Figs. 2–4). While the onset process was a multiday phenomenon, we set the approximate date for onset as 13 June, since by this time CAPE and precipitable water had reached their maxima, while upper-level westerlies had become nearly quiescent. In addition, 13 June was the date after which rainfall was observed on a daily basis in the Marsyandi region.

This time period is consistent with the development and onshore movement of a depression that originated from the Bay of Bengal (Fig. 5), which placed central Nepal under a regime of moist SE flow, consistent with monsoon onset conditions originally discussed by Lang and Barros (2002). Specifically, onset monsoon depressions tend to form over the easterly notch of the monsoon trough over the Bay of Bengal, and propagate westward on the northern flank of the westerly jet over the Indian subcontinent: the more southward the jet, the weaker the interaction with the easterly vertical shear along the Himalayas, keeping the depressions away from the Himalayan range, and favoring disorganized convection over northern India. Accordingly, the 2001 onset depression moved mostly west from the bay, and did not interact as strongly with the mountains as did

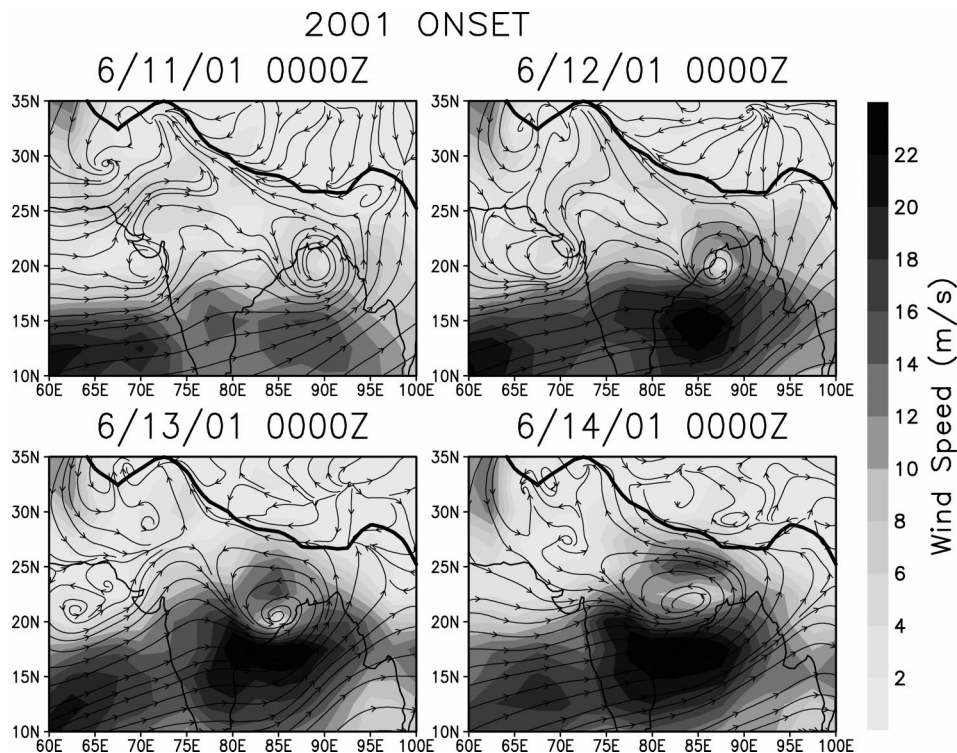


FIG. 5. NCAR–NCEP reanalysis 850-hPa winds at four different times during the 2001 monsoon onset in central Nepal.

the onset depressions from 1999 and 2000 (Lang and Barros 2002). Therefore, although the atmospheric structure exhibited definite change, rainfall totals during the 2001 onset period were not as dramatic as in the previous 2 yr because convection associated with the depression did not reach the mountains. That is, local processes facilitated by the synoptic SE monsoon flow were more important for rainfall during the 2001 onset.

#### 4. Diurnal cycle

While the month-long evolution of the atmosphere was significant during the MOHPREX project, the previous figures also demonstrate the importance of the diurnal cycle. In fact, for many fields (e.g., CAPE) the diurnal cycle was the strongest component of variability. Thus, further analysis of this variability is warranted.

The diurnal cycle of rainfall during June 2001 is shown in Fig. 2b. High- ( $\geq 2000$  m MSL) and low- ( $< 2000$  m MSL) altitude stations were combined and averaged together in 30-min bins to create this plot. Clearly demonstrated is the near-midnight peak in rainfall at both types of stations. Also, there is a lull in rainfall at both stations during the time period 0600–1200 local Nepal time (LNT). Average rain rates increase during the afternoon hours, although there is a significant depression in rainfall near 1800 LNT at high altitudes. The secondary afternoon peak is not as strong during June 2001. This peak tends to be more apparent

at the seasonal scale (Barros et al. 2000), where dominant trends better overcome day-to-day variability.

The methodology employed to calculate the diurnal cycle of sounding-derived variables is reviewed in appendix B. The diurnal cycle of precipitable water is consistent with a late-morning/midday minimum in rainfall and a postmidnight maximum (Fig. 6a). The maximum occurs during the period 2100–0000 LNT and the minimum during 0900–1200 LNT. Soundings that occurred when there was no rainfall (see appendix B) show some differences, with a slight dip of 2 mm at 0000 LNT compared to the all-weather soundings, and a secondary peak of  $\sim 54$  mm at 0300 LNT (not shown).

Figure 6b shows the diurnal cycle of CAPE, which has a similar pattern to precipitable water, reaching a maximum over the period 1800–0000 LNT. This is the 6-h period immediately preceding the nocturnal rainfall peak in the Marsyandi network. The minimum in CAPE occurs during the period 0600–0900 LNT, when observed cloud cover and rainfall were near their minimum. Considering only soundings with no observed rainfall (not shown), there is no significant deviation from this general pattern. Overall, the observations are consistent with a gradual buildup of convective instability during the day, which is then released after midnight leading to a stable atmosphere at the start of a new daytime period. Total column moisture and instability reinforce one another, and from a thermodynamic perspective the nocturnal rainfall peak is no surprise.

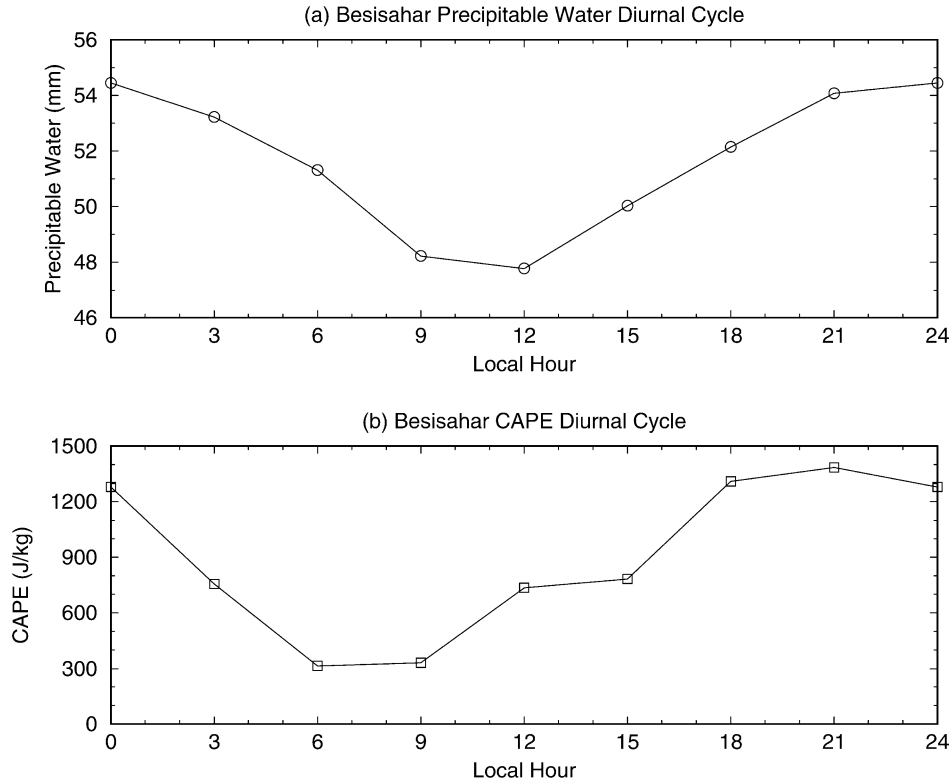


FIG. 6. (a) Diurnal cycle of Besisahar precipitable water. (b) Same as in (a) but for CAPE.

In order to understand this thermodynamic behavior, the diurnal evolution of the vertical profiles of temperature and mixing ratio were explored (not shown). At 0000 LNT, absolute moisture is well above average throughout the depth of the troposphere, while temperatures are slightly cooler than the daily mean, particularly at high altitudes. This is an excellent combination to produce high instability and precipitable water. By contrast, at 1200 LNT, moisture is well below average in the troposphere and temperatures are average to above average. Intermediate times show some variability, but overall reflect the trends between high (0000 LNT) and low atmospheric instability (1200 LNT). What the data suggest is normal diurnal heating and cooling of the atmosphere, which is perhaps lagged a bit by the high moisture levels. Also, there is a daily replenishment of moisture occurring at all levels after the nocturnal depletion. The timing of these two processes leads to the observed diurnal evolution of CAPE and precipitable water.

Note from Fig. 6a that the net daily depletion of atmospheric moisture is  $\sim 6$  mm on average. This moisture supply must be restored daily through local evapotranspiration and through advection by the monsoon flow. Figure 7 shows time series of relative humidity, evapotranspiration, and rainfall at Telbrung (station 19, Fig. 1) during June 2001. The hydrometeorological tower at Telbrung is equipped with sensors that fully monitor the water and energy cycles including soil moisture,

soil temperature, soil heat fluxes, and incoming and outgoing shortwave and longwave radiation fluxes. Evapotranspiration (ET) estimates are obtained indirectly from the latent heat flux, which is estimated as the residual of the energy balance equation. During the monsoon, ET varies between 0.5 and 6 mm day<sup>-1</sup>, corresponding to an average daily evaporative fraction (ET/rainfall) on the order of 0.15. Telbrung is a ridge location; at low elevations, which do not see rainfall during the day, we estimate that the evaporative fraction correspond to average premonsoon values about 0.35 when soil moisture availability is not a limiting factor. Although spatially variable, these data imply that 15%–35% of the daily soil moisture supply is locally or regionally recycled. The remainder must be restored daily through moisture advection by the monsoon flow. Thus, analysis of the diurnal cycle of tropospheric winds is warranted.

Let us consider the diurnal evolution of  $U$  and  $V$  in June 2001 for three surface stations (Fig. 8). The Besisahar station was a temporary station established near the sounding station to support the flights, whereas Koprung and Rambrong are high-altitude stations along the eastern and central ridges, respectively, of the Marsyandi network (Table 1, Fig. 1). There is a diurnal reversal of wind direction at Besisahar (SE during daytime, NW at night) indicative of normal valley flow, although the strongest winds are observed during the daytime. By contrast, Rambrong sees no such reversal, only a slight veering of the enhanced daytime winds

**June 2001 Telbrung [3,168 m]**

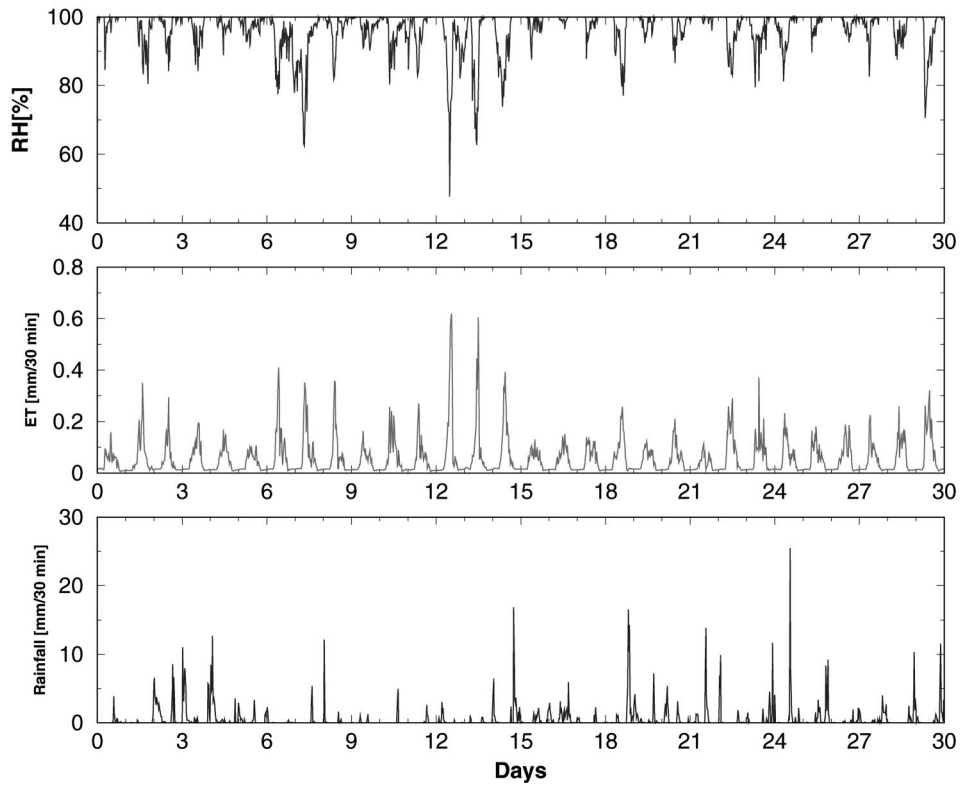


FIG. 7. Time series of (top) relative humidity (RH), (middle) evapotranspiration (ET), and (bottom) rainfall observations at the Telbrung tower (station 19 in Table 1 and Fig. 1) during Jun 2001.

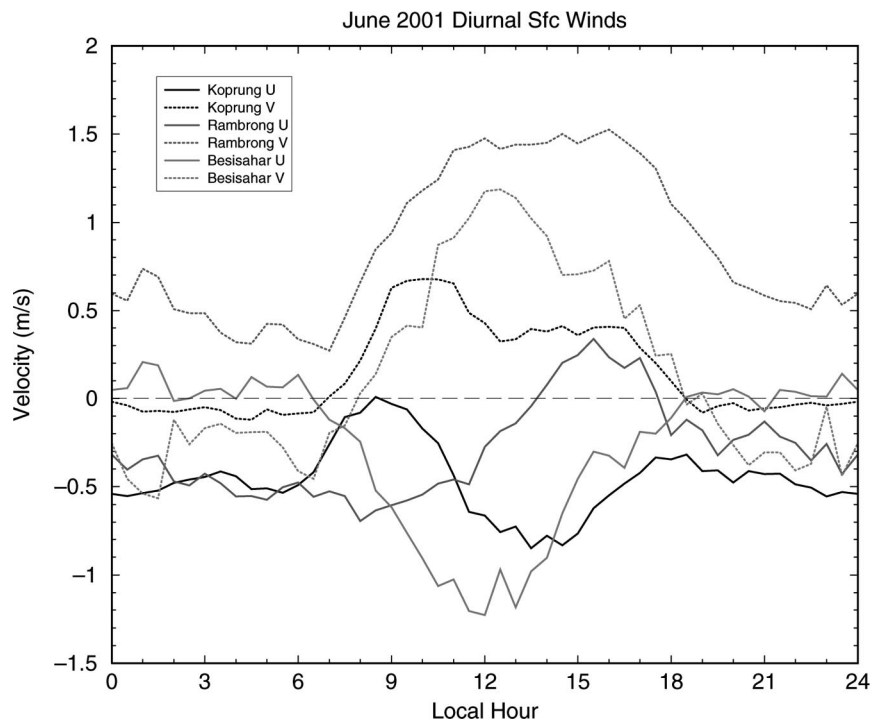


FIG. 8. Daily cycles of surface winds at three network stations.

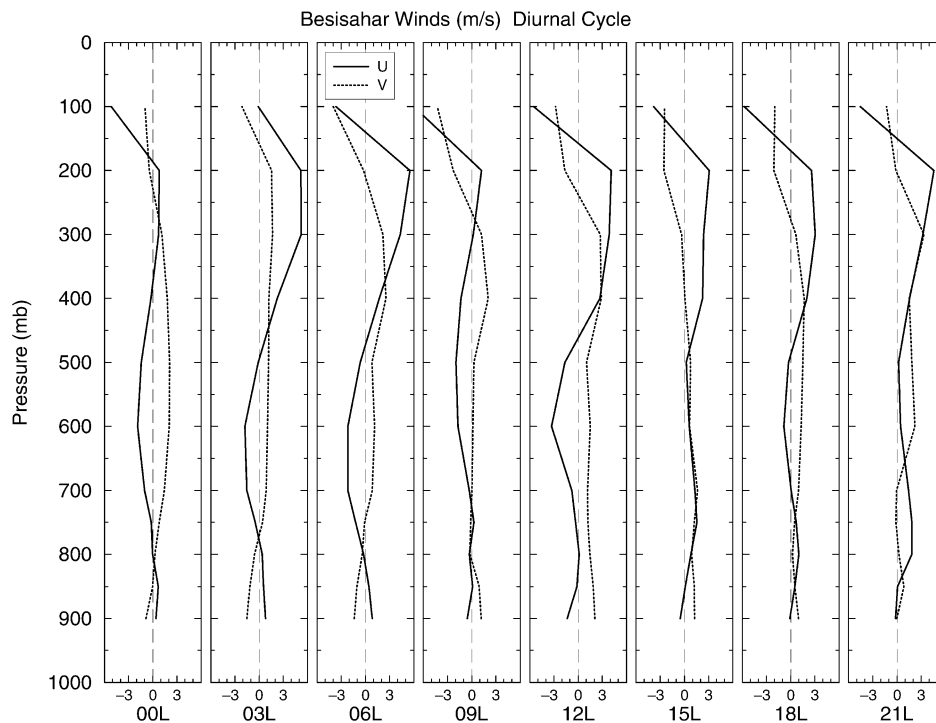


FIG. 9. Daily cycles of vertical profiles of winds at Besisahar.

from SE to SW in the late afternoon. Koprung, at an intermediate altitude, has a very weak reversal in the N–S plane, but once again afternoon winds are strongest and mostly from the S to SE. As noted earlier, the asymmetry between day and night winds is observed elsewhere in the Himalayas (Egger et al. 2000; Ueno et al. 2001; Bollasina et al. 2002).

Figure 9 shows the diurnal evolution of the vertical profiles of  $U$  and  $V$  winds at Besisahar. Mean wind speeds are fairly light ( $<5 \text{ m s}^{-1}$ ) in this region, particularly in the lower troposphere with behavior similar to the surface observations at Besisahar (Fig. 8), that is, daytime upvalley winds and nocturnal downvalley flow. The low-level flow is less southerly/more northerly when results from rain soundings are considered separately (not shown), suggesting that cool outflow from rainstorms increases the downvalley tendency of winds in accord with the analysis of Steiner et al. (2003) in the Alps. The diurnal variability of middle- and upper-tropospheric winds is less clear, mostly showing short-duration fluctuations around the mean trend of increasing westerly flow (i.e., veering of winds) with altitude away from SE flow in the midtroposphere.

The main reason for the lack of an upper-level diurnal cycle is the evolution of the wind fields during the course of the project, which was much stronger than the diurnal cycle amplitude except near the surface (Fig. 3). That is, the most trust should be placed in the diurnal cycle results from the lowest parts of the troposphere, and regions aloft should be viewed skeptically since

temporal evolution of the wind field was not removed when computing diurnal cycle.

These results show that a southerly component of flow is present during much of the day (also observed at high-altitude surface stations; Fig. 8), which is strengthened by the daytime valley wind at low levels. Given the negative gradient in atmospheric moisture between India and the Tibetan Plateau during the monsoon, near-constant advection of moisture into the Marsyandi region is expected under these wind conditions (Peixoto and Oort 1992). Increased near-surface southerly flow during the afternoon enhances this advection and, in concert with the weak nighttime wind reversal, sets up the nocturnal maximum in precipitable water.

### 5. Case study: 13 June 2001

An excellent example of nocturnal convection is the thunderstorm case of 13 June 2001 (local time). While not the most significant rain event during MOHPREX, a TRMM overpass occurred during this storm, providing insight into the vertical structure of nocturnal convection in this region. This storm occurred during the monsoon onset period, when the Bay of Bengal depression was slowly progressing westward across central India. Soundings at 1800 (prior to event) and 2100 UTC (during event) contained 2051 and 2276  $\text{J kg}^{-1}$  of CAPE, respectively, which is suggestive of intense convection (Bluestein 1993). Figure 10 shows rain rates spread out during the night and into the early morning hours for

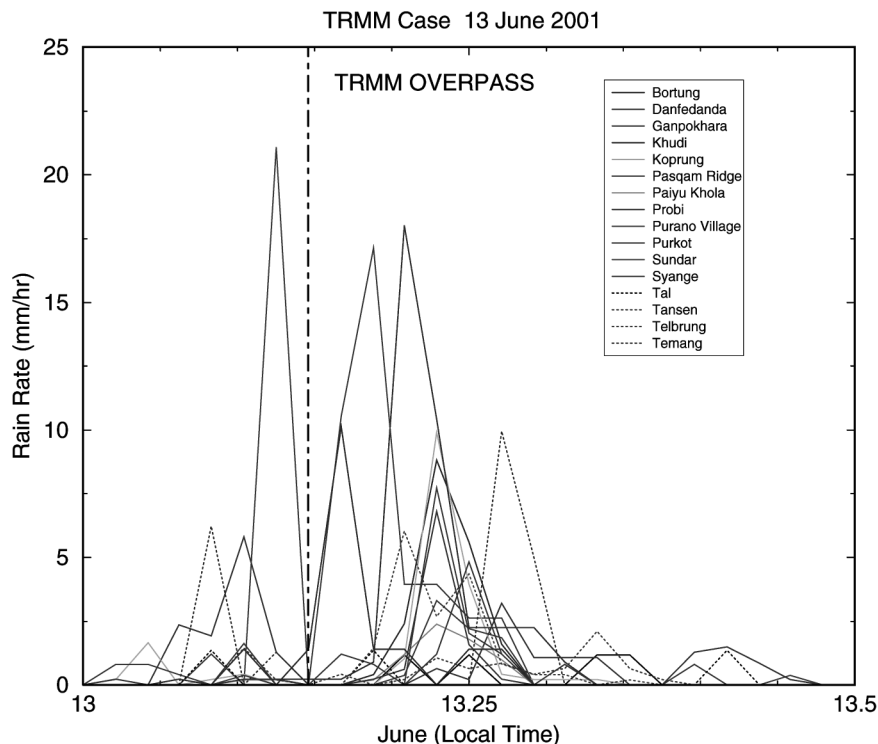


FIG. 10. Time series of rainfall at select network gauges for the nocturnal precipitation event of 13 Jun 2001. The time of the TRMM overpass is noted by the vertical dotted-dashed black line.

available network stations. (Also noted is the time of the TRMM overpass.) The Ganpokhara (central ridge) and Pasqam Ridge stations received the heaviest rainfall. However, rain rates remained less than  $10 \text{ mm h}^{-1}$  at most gauges.

Although the TRMM overpass occurred during a time of reduced rainfall at the network, there was still intense convection in the region (Fig. 11). In fact, during the entire 2100 UTC Besisahar flight, which matched the timing of the TRMM overpass, observers noted light to moderate rainfall. Two vertical cross sections are shown in Fig. 12: one through a core just east of Besisahar (bottom-left panel), and another through the bent line of convection to the SE (bottom-right panel). The Besisahar cell demonstrates the typical vertical structure expected of electrified tropical convection (Petersen et al. 1996). Peak radar reflectivities exceed 45 dBZ, but the highest reflectivities are situated mostly below the freezing-level altitude ( $\sim 5.5 \text{ km MSL}$ ). However, reflectivities in excess of 30 dBZ do extend up to 10 km, well above the  $-10^\circ\text{C}$  layer altitude at  $\sim 7 \text{ km}$ . The threshold of 30 dBZ above the  $-10^\circ\text{C}$  layer altitude is generally regarded as sufficient for electrification (Petersen et al. 1996). Not surprisingly, frequent lightning and thunder were observed at Besisahar.

The SE convective line is much more intense than the Besisahar cell, consistent with its larger size. Indeed, 40 dBZ extends several kilometers above the freezing-level altitude. While a time history of reflectivity struc-

ture is not available, the bent nature of the convective line is suggestive of retarding effects on storm motion by the orography.

*Meteosat-5* infrared imagery (not shown) from this time reveals a classic pattern of nocturnal convection in the Himalayas that is often observed during the monsoon. Strong convection associated with the depression (cf. Fig. 5) is present over central India, while northern India is very clear. However, multiple cells are lined against the Himalayan Mountains, with clear conditions over the Tibetan Plateau.

This case study shows that intense and organized convective systems, isolated from the major monsoon systems over India, can occur along the footslopes of the Himalayas during the monsoon. Such systems can be vertically developed and produce frequent lightning, reminiscent of monsoon break convective storms that have been studied in other regions of the world [e.g., northern Australia; Rutledge et al. (1992), Williams et al. (1992), Cifelli and Rutledge (1998)]. This is consistent with a monsoon that is in its nascent stages, as was the case on 13 June.

## 6. Regional-scale variability

Currently, there are no other radiosonde stations in Nepal, although there are several in northern India, within a few hundred kilometers of the project site. In addition, there are two active radiosonde stations in Tibet

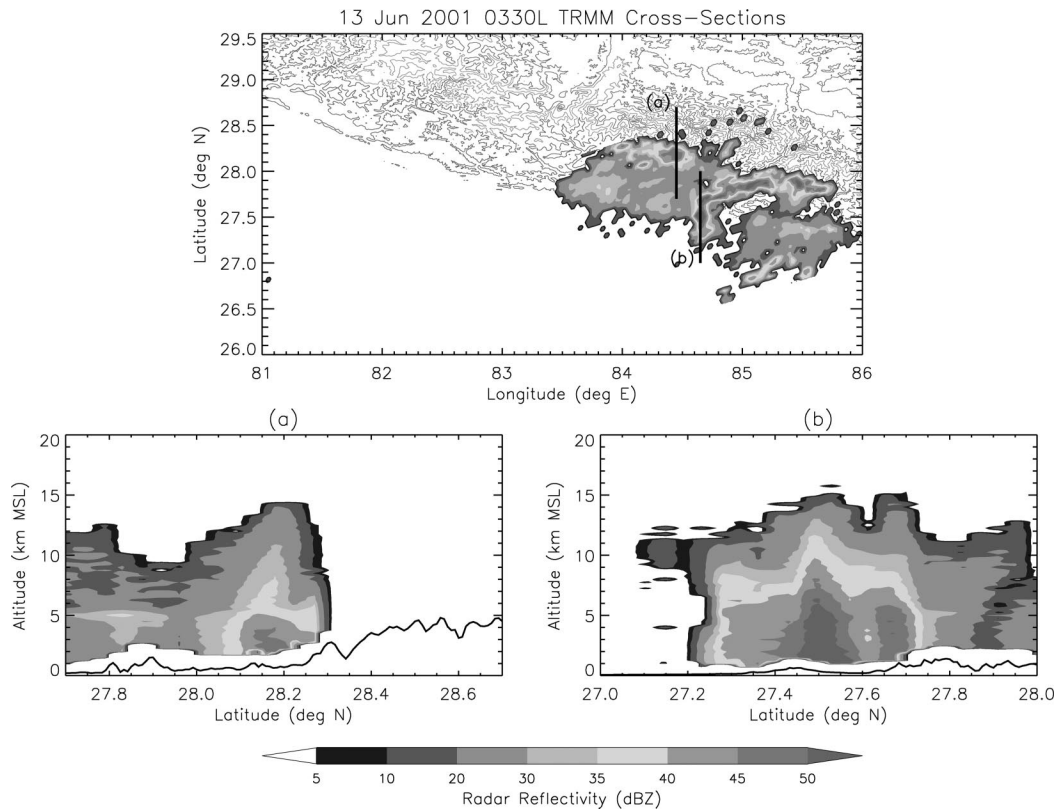


FIG. 11. Horizontal and vertical cross sections of TRMM-measured radar reflectivity for the 13 Jun 2001 event.

(see MB for a map of radiosonde stations in this region). However, soundings from these regions are well known to be among the most error prone in the world (Collins 2001). During our analysis, we found many clearly erroneous winds and temperatures, but by far the largest problem was with the humidity measurements. In the lower troposphere, the air often was measured to be near saturation in the Indian soundings, despite the presence of temperatures in the range  $25^{\circ}$ – $35^{\circ}\text{C}$ . This led to clearly unrealistic mixing ratios greater than  $25\text{ g kg}^{-1}$ . We suspect that wetting of the relative humidity sensor, particularly during rainstorms, is a chronic problem for the Indian flights. The other problem with the soundings were the low frequency of flights (at best two per day; 0000 and 1200 UTC) and frequent early termination before reaching the tropopause, both of which hamper the acquisition of statistically relevant numbers for comparison with the MOHPREX data.

Therefore, in this study we decided to use the National Centers for Environmental Prediction–National Center for Atmospheric Research (NCEP–NCAR) reanalysis (Kalnay et al. 1996) for comparison with MOHPREX. Reanalysis data are available at 6-h intervals,  $2.5^{\circ}$  horizontal resolution, and 12 vertical levels in the range 1000–100 hPa. The caveat is that over the Himalayas, the reanalysis data of interest (temperature, moisture, winds) are of course primarily derived from the aforementioned soundings. However, this is after rigorous

error checking and balancing of any physically unrealistic values by the reanalysis model. The other advantage of using the reanalysis as a basis for comparison is that the scientific community uses it extensively, and thus the MOHPREX data provide an excellent independent check on its ability to capture monsoon conditions near the extreme Himalayan barrier.

Because of the coarse horizontal resolution of the reanalysis data ( $2.5^{\circ}$ ), we do not expect good agreement with the MOHPREX data below the local terrain envelope. The reanalysis cannot possibly resolve the steep mesoscale and microscale terrain features in the vicinity of the MOHPREX launch stations, which would have strong effects on the MOHPREX winds through slope flows and blocking. For example, ridges in excess of 2000–3000 m MSL are located near the valley Besisahar site. Tansen is more exposed near a hilltop, but ridges on the order of 1000–2000 m MSL are nearby. However, above 700 hPa ( $\sim 3000$  m MSL; the local terrain envelope) there is a better basis to compare the NCEP and MOHPREX data, since local terrain would have less of an effect on the dominant large-scale flow at these altitudes. Thus, we place most of our focus on middle- and upper-tropospheric data and determine how well the reanalysis matches the large-scale environment in the Himalayas.

The first step is to compare the Besisahar and Tansen soundings themselves, to understand variability on the

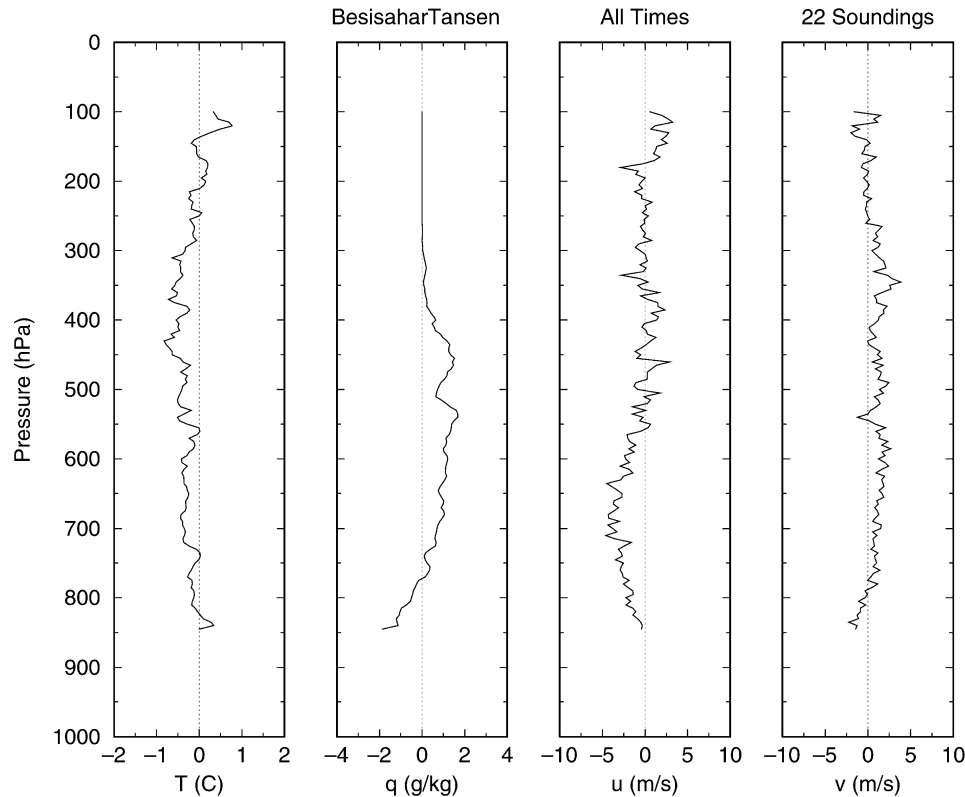


FIG. 12. Vertical profiles of mean temperature, mixing ratio, and wind differences between Besisahar and Tansen.

mesoscale (physical separation of the sites is  $\sim 90$  km). For all comparisons in this section soundings were first interpolated to a vertical grid with 5-hPa spacing. Figure 12 shows the mean profile differences between the two sites for all relevant parameters. The sites had 22 soundings in common with one another. On the whole, agreement is fairly good, suggesting not much atmospheric variability is occurring on the mesoscale near the mountains. There is a tendency for the Besisahar profile to be slightly cooler ( $<1^{\circ}\text{C}$  difference) than Tansen.

Tansen saw greater moisture in the lower troposphere, possibly due to the presence of surface vegetation at the elevated launch site ( $\sim 850$  hPa altitude). However, there was significantly more moisture ( $\sim 2$  g  $\text{kg}^{-1}$  difference) in the midtroposphere above Besisahar. One reason for this may have been the larger percentage of rain flights

at Besisahar, leading to its sondes traveling through more cloud layers. However, another possibility could be enhanced moisture convergence at midlevels due to the blocking effects of the Himalayan range. At Besisahar there is a tendency for stronger low-level easterly winds, as well as more southerly flow throughout the troposphere (except near the surface). The low-level wind effects are most likely the result of the Besisahar valley wind.

In comparing the NCEP–NCAR reanalysis to MOHPREX, we decided on five grid points for this intercomparison (Fig. 1; Table 3): two at  $30.0^{\circ}\text{N}$  in the Tibetan Plateau (points A and B), to the NW and NE; two along the Himalayas at  $27.5^{\circ}\text{N}$  (points C and D), to the east and west of the launch sites; plus one at  $25.0^{\circ}\text{N}$  on the Indian plains SE of the project site (point E). Table 3 shows the relevant information for these grid points.

There is good agreement in the wind time series at high levels in the atmosphere (Fig. 13a). At 500 hPa (Fig. 13b), above the tips of the ridges by Besisahar,  $U$  winds match well with nearby grid points (points C and D). However, the reanalysis shows more variability than the MOHPREX data. Note how the late June increase in  $V$  wind at Besisahar is not captured as well by the reanalysis. Perhaps the best agreement between MOHPREX and the reanalysis is seen at 200 hPa (Fig. 13b), well above the tallest ridges. Here the changes at Be-

TABLE 3. Specifics of the NCEP–NCAR reanalysis grid points used in the analyses. Note that the elevation is for model topography only, and does not necessarily match the true elevation at that location on Earth.

Letter	Lat ( $^{\circ}\text{N}$ )	Lon ( $^{\circ}\text{E}$ )	Elev (MSL, m)	Description
A	30.0	82.5	4351	Plateau
B	30.0	85.0	5397	Plateau
C	27.5	82.5	858	Himalayas
D	27.5	85.0	1966	Himalayas
E	25.0	85.0	-115	Plains

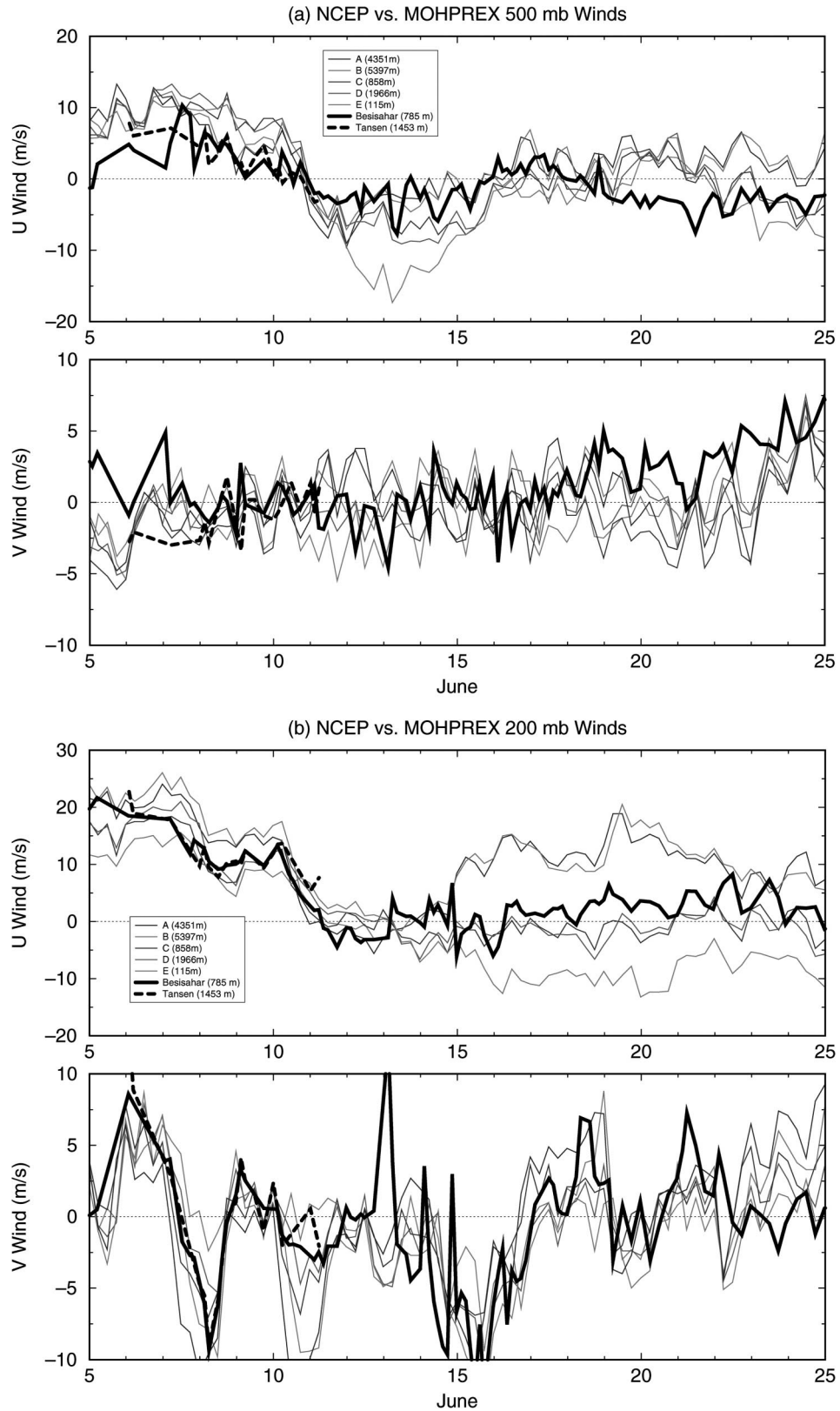


FIG. 13. (a) Time series of 500-hPa winds for Besisahar, Tansen, and five surrounding NCEP-NCAR reanalysis grid points (Table 3). (b) Same as in (a) but for 200 hPa.

sisahar and Tansen reflected the large-scale variability occurring in the NCEP data. In particular, note how once the monsoon was fully established after 15 June, differences in the  $U$  data occurred among the grid points. A reintensification of the westerlies occurs in the Tibetan Plateau, while in northern India upper-level easterlies were dominant. This pattern is indicative of the familiar upper-level monsoon high over the plateau (Murakami 1987). In between, weak E–W flow becomes established in the Himalayan grid points (C and D) and Besisahar.

Mean differences in temperature, moisture, and wind profiles are shown in Fig. 14a (Besisahar–NCEP) and Fig. 14b (Tansen–NCEP). We display characteristic terrain elevations in these plots to assist in understanding terrain influences. Most ridges in the immediate vicinity of the MOHPREX radiosonde sites do not exceed 2000–3000 m MSL, although 4000–5000 m are common elevations in the nearby high Himalayas and Tibetan Plateau. Note how both Besisahar and Tansen tended to have more midlevel moisture than the NCEP grid points. In addition, temperature profiles disagreed the most for the Tibetan grid points as expected since the plateau is an elevated heat source relative to the surrounding atmosphere (e.g., Ye 1981). As seen in the wind time series, the best agreement between MOHPREX and the reanalysis occurred for the Himalayan grid points. However, there still tended to be stronger southerly flow at Besisahar, throughout much of the troposphere. This could have been due to the N–S valley in which the site was located. Flow in the N–S plane through this valley would be less obstructed than flow over the coarse reanalysis topography. There also could have been some channeling of the flow by the narrow valley, increasing wind speeds. This would increase moisture advection and may be a partial cause of the observed large differences in midlevel moisture.

The midlevel moisture differences have profound impacts on total column moisture. Figure 15 shows time series of precipitable water for the reanalysis points and for MOHPREX (cf. Fig. 4a). While PW at Tansen agrees relatively well (within  $\sim 25\%$ ) with the moisture amounts at the closest NCEP grid point (point C), Besisahar has much more moisture, at times even exceeding the precipitable water at the upstream NCEP grid point over northern India (point E). Most NCEP profiles capture the decreasing moisture in early June, but the increase associated with monsoon onset comes up to 4 days later than during MOHPREX. In addition, there is a late June moisture decrease in most of the NCEP data that was not observed at Besisahar. Finally, despite having four time points per day the NCEP data show a diurnal cycle that is extremely weak compared to the one observed at Besisahar. Overall, there appear to be profound disagreements between the MOHPREX and reanalysis data in terms of atmospheric moisture.

According to the reanalysis, average June 2001 daily rainfall in the vicinity of the Marsyandi network (using

point D) was 12.3 mm, compared to the 17–19 mm observed on an average day at the network proper. Indeed, the observed range of rainfall totals at the network is comparable to reanalysis-predicted rainfall on the outskirts of the Bay of Bengal. This is also true for precipitable water values. Clearly, significantly more moisture exists along the Himalayas than previously estimated.

## 7. Conclusions

The MOHPREX project has been described, and major results shown. The project was a great success considering the difficulties experienced. Good coverage of the diurnal cycle of the atmosphere (temperature, moisture, winds), as well as the onset and development of the early monsoon, were obtained for two sites along the Himalayas in central Nepal.

The onset of the monsoon manifested itself as a gradual increase in total column moisture and convective instability, and a weakening of middle- and upper-tropospheric westerly winds. The lower-level winds were more strongly affected by the diurnal cycle of slope and valley winds. However, daytime upslope/upvalley winds were more intense than their nocturnal downslope/downvalley counterparts. This result is consistent with observations in other parts of the Himalayas (Egger et al. 2000; Ueno et al. 2001; Bollasina et al. 2002) and supports the theory of diurnal winds along tropical slopes in opposing flows (Fitzjarrald 1984). In this case, the opposing flow is the monsoon winds. Also, the observations are consistent with the presence of the Tibetan surface low pressure (Murakami 1987), which would tend to favor upslope flow over downslope (Zängl et al. 2001).

The diurnal cycles of moisture and instability support the observations of a postmidnight maximum in rainfall in this region. A case study of a nocturnal storm was shown, with intense vertical structure as revealed by TRMM. The data suggest that vertically intense break convection was prevalent during the early monsoon, consistent with a monsoon flow that had not fully established itself by the end of the project in late June.

Based on the results of the MOHPREX project, a possible mechanism to explain the nocturnal peak in rainfall is shown in Fig. 16. Large-scale monsoon flow is presumed to be roughly constant during the day and night, though it is of course subject to the variability in the monsoon trough over northern India and the appearance of monsoon depressions in the Bay of Bengal. The Besisahar wind data show weak diurnal variation well above the surface, which supports this assumption. However, the mountains provide a huge barrier to these flows, tending to block them and cause convergence, particularly at low levels. This convergence is reduced during the daytime because diurnally forced upslope and upvalley flow reduce the spatial gradients in wind velocities. The upslope flow aids the formation of con-

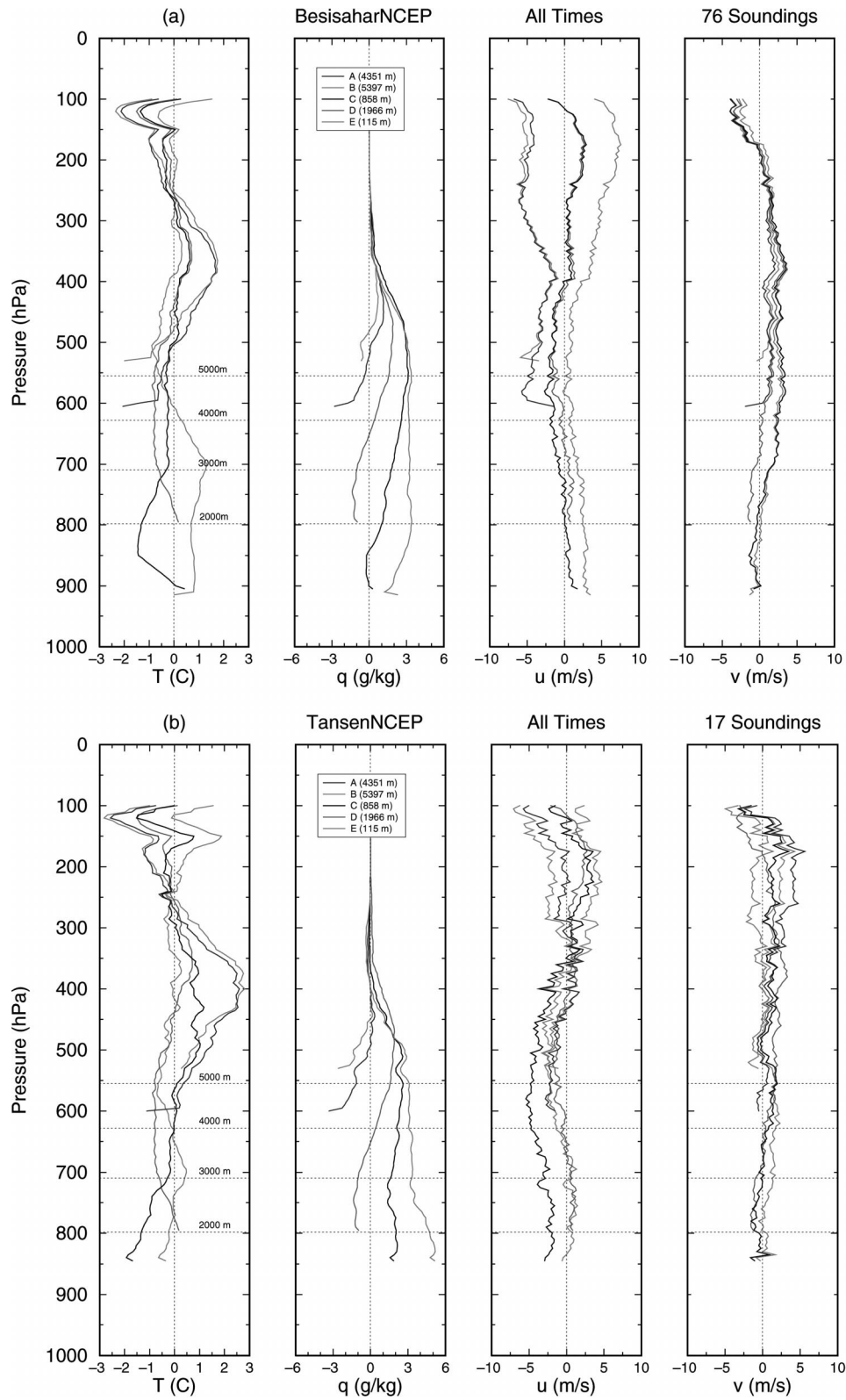


FIG. 14. (a) Vertical profiles of mean temperature, mixing ratio, and wind differences between Besisahar and five surrounding NCEP–NCAR reanalysis grid points. (b) Same as in (a) but for Tansen and the reanalysis grid points. The horizontal dotted lines note the pressure-coordinate heights of characteristic terrain elevations near Besisahar and Tansen (2000–5000 m MSL).

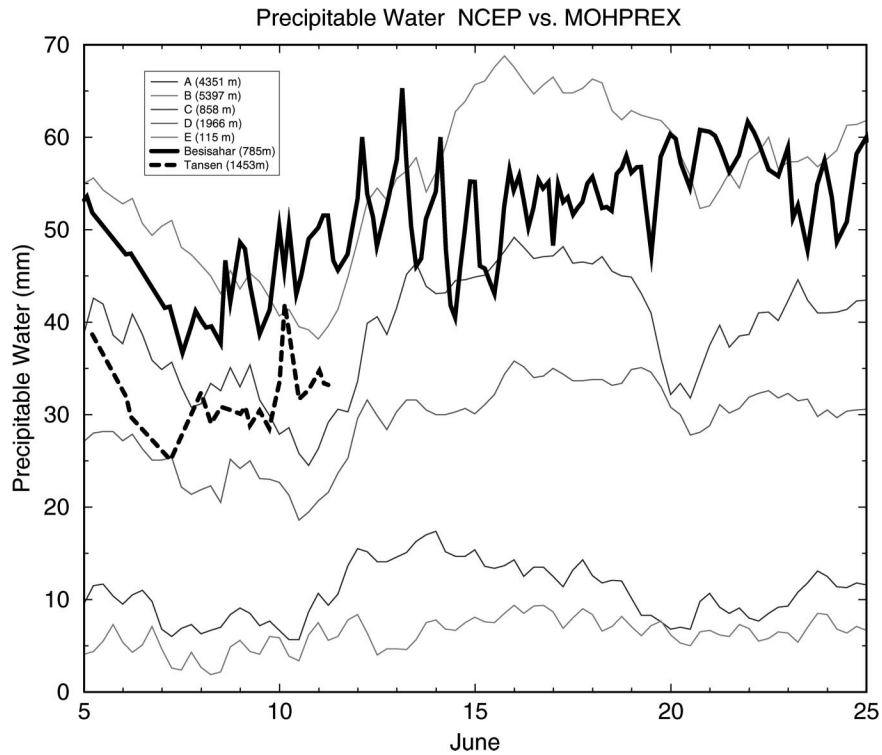


FIG. 15. Time series of precipitable water for Besisahar, Tansen, and five surrounding NCEP–NCAR reanalysis grid points.

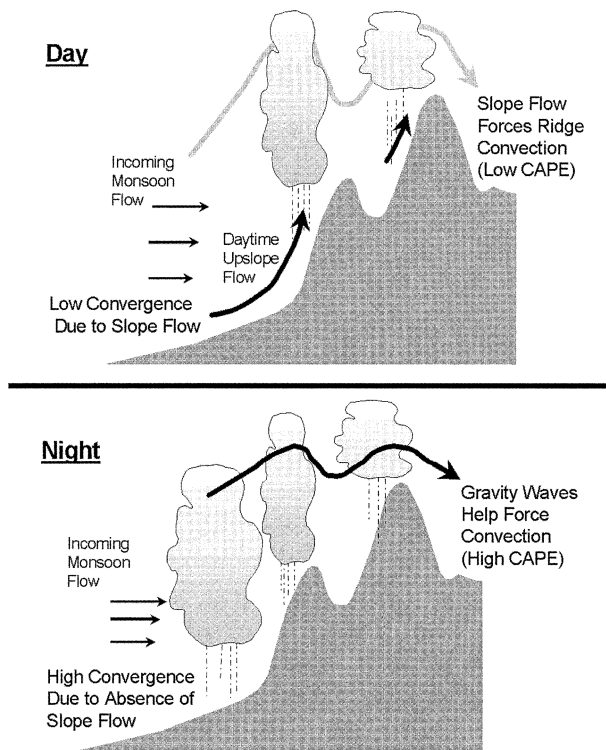


FIG. 16. Schematic diagram of the proposed mechanism to explain nocturnal rainfall in the Himalayas.

vection at higher elevations, leading to the observed secondary peak in rainfall there.

At night, however, wind speeds become relatively weak near the surface, even reversing direction in valleys such as the Marsyandi. Thus, near-surface wind convergence increases, leading to upward motion that can force convection. This convection is aided by the steady increase of moisture during the day from advection by the monsoon flow. In addition, atmospheric instability is maximized during nocturnal hours, due to interaction between the steady increase in surface moisture and diurnal heating and cooling of the atmosphere. The near-coincident availability of moisture, instability, and surface forcing leads to the nocturnal peak in rainfall. This peak will be strongest at low elevations where blocking of flow is most active, as observed.

This is qualitatively similar to the processes that cause predominantly nocturnal rainfall over tropical islands, such as Hawaii (Chen and Nash 1994). On tropical islands and in the Himalayas, the thermally forced diurnal flow interacts with the predominant environmental flow (trade winds in the case of Hawaii, the monsoon flow for the Himalayas), causing nocturnal convergence and subsequent precipitation.

The nocturnal convergence could be aided by the interaction between mountain-forced gravity waves and the thermodynamics of the Himalayan atmosphere, which MOHPREX shows is most favorable for noctur-

nal convection. In a numerical simulation of monsoon onset in this region, Barros and Lang (2003) showed that spatially fixed gravity waves form over the terrain, with downward motion strongest over ridges and upward motion strongest between ridges. Under normal monsoon conditions, the SE flow that creates this gravity wave pattern is not as strong, but it should be enough to force some waves. The waves occur as long as the forcing flow holds, and the upward-moving antinodes should fire off convection when the thermodynamics are favorable (near midnight).

In summary, the proposed mechanism suggests a robust atmospheric system that strongly favors nocturnal convection and rainfall. It also explains why this nocturnal peak does not occur elsewhere, such as the Tibetan Plateau or the northern Indian plains, and why this nocturnal peak only occurs during the monsoon. The interaction of the ambient monsoon flow with the south slopes of the Himalayas, modulated by the diurnal variability of atmospheric state, is the primary cause of the nocturnal peak. Future numerical modeling work is planned to provide more support for this hypothesis.

This hypothesis has advantages over one based on a low-level jet (LLJ), which is used to explain nocturnal convection in the high plains of the United States (e.g., Bluestein 1993). Although LLJs are expected to occur near large mountain barriers at latitudes characteristic of the Himalayas ( $\sim 30^\circ$ ), we find no evidence for diurnally variable barrier jets in either the MOHPREX or NCEP–NCAR reanalysis data. The Himalayas are a data-poor region, but strong LLJs may be prevented from forming in the vicinity of the Marsyandi network (and other portions of the middle Himalayas) due to the steep and variable topography in this region. In addition, the long-term presence of the monsoon trough over northern India may play a role in preventing or altering LLJs. Synoptically forced barrier jets, however, can be important for moisture and precipitation when monsoon depressions approach the Himalayas (Fig. 5; also Lang and Barros 2002). However, under these conditions the large-scale flow tends to overwhelm any terrain-forced diurnal effects (Lang and Barros 2002).

The MOHPREX data provided an excellent independent check on the performance of the NCEP–NCAR reanalysis in this normally data-poor region. Overall, the reanalysis data captured well upper-level winds that would not be as affected by the steep topography that the model is too coarse to resolve. However, moisture was consistently underestimated by the reanalysis, having profound impacts on simulated rainfall amounts, which undercut observed values by about one-third. The low model resolution and lack of reliable observations in this region are the most likely candidates to explain this underestimation of moisture.

Overall, it appears that the south slopes of the Himalayas still are not well resolved by existing datasets, despite the presence of prodigious monsoon rainfall and latent heating. The results of MOHPREX and from the

Marsyandi network in general should go a long way toward addressing these concerns. These data are being used currently to evaluate simulations produced by a cloud-resolving atmospheric model under typical monsoon onset conditions in the central Himalayas. The objective is to elucidate the orographic effects on the spatial distribution of winds and rainfall, and to characterize orography–convection interactions and their impact on the diurnal cycle of rainfall in the Himalayas.

*Acknowledgments.* NSF provided funding for MOHPREX under Grant EAR-9909498. Several participants were also funded by NASA/TRMM under Grant NAG5-7781. Dr. Ana Barros was the principal investigator for MOHPREX. Dr. Timothy Lang was the lead scientist in the field during the project. The authors extend their gratitude to the Nepal Department of Hydrology and Meteorology for the opportunity to conduct the MOHPREX project. This project could not have been possible without the dedicated efforts of Tank Ojha, our Nepalese liaison, and his network of interpreters, porters, and drivers. Dr. Jaakko Putkonen of the University of Washington participated in the first 2 weeks of the field phase of MOHPREX, and manages the periodic collection of Marsyandi network data at other times. Timothy Lim of NCAR was the lead technician in the field for the first 2 weeks of the project, and was responsible for training project participants in the launching of radiosondes. We thank the graduate and undergraduate students who assisted in the field: Dr. Steve Nesbitt (University of Utah) and Casey Brown (Harvard University), as well as Elizabeth Korb and Martha Fernandes (both of Tufts University). Dr. Rit Carbonne and Ned Chamberlain of NCAR, and Dr. Douglas Burbank and Beth Pratt of University of California, Santa Barbara, assisted in the planning of MOHPREX. Dr. Ramata Magagi of Harvard University provided a very useful *Meteosat-5* perspective via satellite phone during the project (satellite data were obtained from the University of Wisconsin/SSEC). Dr. Edward Zipser of University of Utah gave excellent feedback and guidance in the interpretation of results. Finally, the staff and ownership of the Hotel Sayapatri in Besisahar are commended for their exceptional hospitality toward project workers.

## APPENDIX A

### Sounding Data Quality Control

The radiosonde system used was the National Center for Atmospheric Research (NCAR) GPS/Loran Atmospheric Sounding System (GLASS). The radiosonde model used was the Vaisala RS 80-15GH. Both of these systems are standards within the meteorological research community, and more information on them (including specifications and measurement accuracy) can be found at the NCAR Atmospheric Technology Division Web site (<http://www.atd.ucar.edu/rtf/facilities/>

class/class.html). The GLASS system provides excellent vertical resolution with a time resolution of  $\sim 1$  s. Winds are measured by the GPS method.

There were 150 sondes originally supplied to the MOHPREX project. However, as is typical of similar field projects, some attrition in the form of launch failures and data loss occurred. Nevertheless, launch failures were typical to below average as compared to other field experiments with the NCAR GLASS system (T. Lim 2001, personal communication). Specifically, launch failures were about 10%–15% of all sondes, most of these being partial failures with some (often most) data available. There were 121 sounding flights of analyzable quality for Besisahar (117 with at least some wind data), and 22 for Tansen (21 with at least some wind data; Table 2). Corrupted data were removed by a combination of standard hydrostatic checks and checks on erratic raw data at the timescale of 1 s. Corrected profiles were carefully checked against less noisy flights at similar times in order to confirm that the proper data were retained. No obvious biases in observed fields were noted.

## APPENDIX B

### Diurnal Cycle Analysis

There were not enough soundings to compute a diurnal cycle at Tansen with acceptable statistical confidence in the results. Diurnal cycles for Besisahar soundings were calculated in the following way. First, the day in local time was split up into eight 3-h bins (0000, 0300, 0600, 0900, 1200, 1500, 1800 and 2100 LNT). Then, soundings were placed in the appropriate bin if they occurred within 1.5 h of the bin time. Once all soundings were distributed, mean values of all fields were calculated for each bin. Because Nepal is nearly 6 h ahead of UTC and launches were based on UTC time, flights did not deviate significantly from the center of the bin period except when they were adjusted to match TRMM overpasses. Note from Table 2 that only 11 of 23 project days had more than five launches, and only 6 days had seven or more launches. The most common off hours were 0900, 1500, and 2100 LNT, so results from these time periods should be viewed with extra caution, as fewer flights were available for analysis. Diurnal cycle analyses do not take into account the month-long evolution of the analyzed fields, which was discussed in section 3.

Daily cycles of vertical profiles were calculated by first dividing up each vertical profile into 11 segments. Resolution of each segment was 50 hPa between 900 and 700 hPa, and 100-hPa resolution above this layer up to 100 hPa. For any specific flight, all data within each segment were averaged together. Then, each segment was binned in time and the daily cycle calculated in the manner discussed above.

In order to determine the extent to which the presence

of rain affected results, rain and no-rain flights also were defined. Rain flights were those that occurred with rainfall observed at the surface, either at the time of launch, up to 1 h prior to launch, or within 15 min after launch. The main purpose was to identify soundings that occurred when the lower troposphere was potentially rain saturated, which could significantly affect low-level moisture measurements (and throw off estimates of CAPE and PW).

## REFERENCES

- Banta, R. M., 1990: The role of mountain flows in making clouds. *Atmospheric Processes over Complex Terrain, Meteor. Monogr.*, No. 45, Amer. Meteor. Soc., 229–283.
- Barros, A. P., and T. J. Lang, 2003: Exploring spatial modes of variability of terrain–atmosphere interactions in the Himalayas during monsoon onset. Hydrosocieties Rep. Series 03-001, Division of Engineering and Applied Sciences, Harvard University, 51 pp.
- , M. Joshi, J. Putkonen, and D. W. Burbank, 2000: A study of the 1999 monsoon rainfall in a mountainous region in central Nepal using TRMM products and rain gauge observations. *Geophys. Res. Lett.*, **27**, 3683–3686.
- Bluestein, H. B., 1993: *Observations and Theory of Weather Systems*. Vol. II. *Synoptic–Dynamic Meteorology in Midlatitudes*, Oxford University Press, 594 pp.
- Bollasina, M., L. Bertolani, and G. Tartari, 2002: Meteorological observations at high altitude in the Khumbu Valley, Nepal Himalayas, 1994–1999. *Bull. Glaciol. Res.*, **19**, 1–11.
- Burbank, D. W., and N. Pinter, 1999: Landscape evolution: The interactions of tectonics and surface processes. *Basin Res.*, **11**, 1–6.
- Chen, L., E. R. Reiter, and Z. Feng, 1985: The atmospheric heat source over the Tibetan Plateau: May–August 1979. *Mon. Wea. Rev.*, **113**, 1771–1790.
- Chen, Y.-L., and A. J. Nash, 1994: Diurnal variation of surface airflow and rainfall frequencies on the island of Hawaii. *Mon. Wea. Rev.*, **122**, 34–56.
- Cifelli, R., and S. A. Rutledge, 1998: Vertical motion, diabatic heating, and rainfall characteristics in north Australia convective systems. *Quart. J. Roy. Meteor. Soc.*, **124**, 1133–1162.
- Collins, W. G., 2001: The operational complex quality control of radiosonde heights and temperatures at the National Centers for Environmental Prediction. Part II: Examples of error diagnosis and correction from operational use. *J. Appl. Meteor.*, **40**, 152–168.
- Egger, J., S. Bajrachaya, U. Egger, R. Heinrich, J. Reuder, P. Shayka, H. Wendt, and V. Wirth, 2000: Diurnal winds in the Himalayan Kali Gandaki valley. Part I: Observations. *Mon. Wea. Rev.*, **128**, 1106–1122.
- EUMETSAT, 2000: The Meteosat System. EUM TD 05, European Organisation for the Exploitation of Meteorological Satellites.
- Fitzjarrald, D. R., 1984: Katabatic wind in opposing flow. *J. Atmos. Sci.*, **41**, 1143–1158.
- He, H., J. W. McGinnis, Z. Song, and M. Yanai, 1987: Onset of the Asian monsoon in 1979 and the effect of the Tibetan Plateau. *Mon. Wea. Rev.*, **115**, 1966–1995.
- Kalnay, E., and Coauthors, 1996: The NCEP/NCAR 40-Year Reanalysis Project. *Bull. Amer. Meteor. Soc.*, **77**, 437–471.
- Krishnamurti, T. N., and C. M. Kishitawal, 2000: A pronounced continental-scale diurnal mode of the Asian summer monsoon. *Mon. Wea. Rev.*, **128**, 462–473.
- Kummerow, C., W. Barnes, T. Kozu, J. Shiue, and J. Simpson, 1998: The Tropical Rainfall Measuring Mission (TRMM) sensor package. *J. Atmos. Oceanic Technol.*, **15**, 809–816.
- Kuo, H. L., and Y. F. Qian, 1981: Influence of the Tibetan Plateau on cumulative and diurnal changes of weather and climate in summer. *Mon. Wea. Rev.*, **119**, 2337–2356.

- Lang, T. J., and A. P. Barros, 2002: An investigation of the onsets of the 1999 and 2000 monsoons in central Nepal. *Mon. Wea. Rev.*, **130**, 1299–1316.
- Li, C., and M. Yanai, 1996: The onset and interannual variability of the Asian summer monsoon in relation to land–sea thermal contrast. *J. Climate*, **9**, 358–375.
- Luo, H., and M. Yanai, 1983: The large-scale circulation and heat sources over the Tibetan Plateau and surrounding areas during the early summer of 1979. Part I: Precipitation and kinematic analyses. *Mon. Wea. Rev.*, **111**, 922–944.
- , and —, 1984: The large-scale circulation and heat sources over the Tibetan Plateau and surrounding areas during the early summer of 1979. Part II: Heat and moisture budgets. *Mon. Wea. Rev.*, **112**, 966–989.
- Magagi, R., and A. P. Barros, 2003: Latent heating of rainfall during the onset of the Indian Monsoon using TRMM-PR and radio-sonde data. Hydrosciences Rep. Series 03-002, Division of Engineering and Applied Sciences, Harvard University, 56 pp.
- Moncrieff, M. W., and M. J. Miller, 1976: The dynamics and simulation of tropical cumulonimbus and squall lines. *Quart. J. Roy. Meteor. Soc.*, **102**, 373–394.
- Murakami, T., 1987: Orography and monsoons. *Monsoons*, J. S. Fein and P. L. Stephens, Eds., John Wiley and Sons, 331–364.
- Ohsawa, T., H. Ueda, T. Hayashi, A. Watanabe, and J. Matsumoto, 2001: Diurnal variations of convective activity and rainfall in tropical Asia. *J. Meteor. Soc. Japan*, **79**, 333–352.
- Peixoto, J. P., and A. H. Oort, 1992: *Physics of Climate*. American Institute of Physics, 520 pp.
- Petersen, W. A., S. A. Rutledge, and R. E. Orville, 1996: Cloud-to-ground lightning observations from TOGA COARE: Selected results and lightning location algorithms. *Mon. Wea. Rev.*, **124**, 602–620.
- Rutledge, S. A., E. R. Williams, and T. D. Keenan, 1992: The Down Under Doppler and Electricity Experiment (DUNDEE): Overview and preliminary results. *Bull. Amer. Meteor. Soc.*, **73**, 3–16.
- Shrestha, A. B., C. P. Wake, J. E. Dibb, and P. A. Mayewski, 2000: Precipitation fluctuations in the Nepal Himalaya and its vicinity and relationship with some large scale climatological parameters. *Int. J. Climatol.*, **20**, 317–327.
- Shrestha, M. L., 2000: Interannual variation of summer monsoon rainfall over Nepal and its relation to the Southern Oscillation index. *Meteor. Atmos. Phys.*, **75**, 21–28.
- Steiner, M., O. Bousquet, R. A. Houze Jr., B. F. Smull, and M. Mancini, 2003: Airflow within major alpine river valleys under heavy rainfall. *Quart. J. Roy. Meteor. Soc.*, **129**, 411–432.
- Ueno, K., and Coauthors, 2001: Meteorological observations during 1994–2000 at the Automatic Weather Station (GEN-AWS) in Khumbu region, Nepal Himalayas. *Bull. Glaciol. Res.*, **18**, 23–30.
- Williams, E. R., S. A. Rutledge, S. C. Geotis, N. Renno, E. Rasmussen, and T. Rickenbach, 1992: A radar and electrical study of tropical hot towers. *J. Atmos. Sci.*, **49**, 1386–1395.
- Wu, G., and Y. Zhang, 1998: Tibetan Plateau forcing and the timing of the monsoon onset over south Asia and the South China Sea. *Mon. Wea. Rev.*, **126**, 913–927.
- Yatagai, A., 2001: Three-dimensional features of summer monsoon precipitation seen from TRMM/PR and latent heat release over south Asia. Albuquerque, NM, Amer. Meteor. Soc., Preprints, *Symp. on Precipitation Extremes: Prediction, Impacts, and Responses*, Albuquerque, NM, Amer. Meteor. Soc., 195–198.
- Ye, D., 1981: Some characteristics of the summer circulation over the Qinghai-Xizang (Tibet) Plateau and its neighborhood. *Bull. Amer. Meteor. Soc.*, **62**, 14–19.
- Zängl, G., J. Egger, and V. Wirth, 2001: Diurnal winds in the Himalayan Kali Gandaki valley. Part II: Modeling. *Mon. Wea. Rev.*, **129**, 1062–1080.